J Mater Sci (2012) 47:999–1003
DOI 10.1007/s10853-011-5879-8

Synthesis and capacitive property of δ-MnO_2 with large surface area

Xin Zhang · Xiaopei Chang · Na Chen · Kuan Wang · Liping Kang · Zong-huai Liu

Received: 28 June 2011 / Accepted: 16 August 2011 / Published online: 31 August 2011

Abstract δ-MnO_2 with layered structure is synthesized in a mixed system of $KMnO_4$ and C_3H_6O (epoxypropane) by a facile low-temperature hydrothermal method at 90 °C for 24 h. The obtained product is characterized by X-ray diffraction (XRD), scanning electron microscopy, transmission electron microscopy, and N_2 adsorption–desorption, and its electrochemical property was investigated by cyclic voltammetry method. Experiment results show that the as-synthesized product has a layered structure and a high specific surface area of 188 $m^2\ g^{-1}$, and C_3H_6O existing in the reaction system plays a crucial role for the formation of δ-MnO_2 particles. Electrochemical characterization indicates that the prepared material exhibits an ideal capacitive behavior with the initial capacitance value of 296 F g^{-1} in 1 mol L^{-1} Na_2SO_4 aqueous solution at a scan rate of 5 mV s^{-1} and good cycling behavior.

Introduction

Recent years, the electrochemical capacitor as a charge-storage device has aroused great attention, and it can be used in the electric vehicles, power sources, and electronic devices due to its high energy storage ability, high power output, and high cycle capacity [1–3]. Research results show that the capacity of the electrochemical capacitor is highly connected with its cathode materials, three types of which such as various forms of carbon, transition metal oxides, and conducting polymers have been widely researched [4–6]. Among all these materials, manganese oxide has been conceived as a promising supercapacitive material because of its low cost, high electrochemical activity, and being friendly with nature environmental [7, 8].

Manganese oxides can be existed as α, β, γ, δ, and λ types due to the different link ways of the basic unit [MnO_6] octahedra. α, β, and γ-type manganese oxides possess 1D tunnel structure, while δ-type manganese oxide shows a 2D layered one [9, 10]. In general, the specific capacitance of the cathode materials is related to its specific surface area, the electrical conductivity in the solid phase, and ionic transport within the pores because the larger specific surface area and good ionic transportation can lead to a higher current density and facilitate the fast transport of electrolyte with metal ions [11]. In this regard, a layered structure consisting of bicontinuous networks of solid and pores on the nanometer scale is an attractive candidate for application as active electrode material, and especially in the mesoporous birnessite-type manganese oxide with large specific surface area [12]. Up to now, δ-type manganese oxides with layered structure have been fabricated via electrochemical and chemical routes, and their electrochemical properties have been investigated [13]. The investigated materials mainly focus on the amorphous or poorly crystallized manganese oxides, manganese oxide thin films. The research results indicate that manganese dioxide powders have shown an average

Electronic supplementary material The online version of this article (doi:10.1007/s10853-011-5879-8) contains supplementary material, which is available to authorized users.

X. Zhang · X. Chang · N. Chen · K. Wang · L. Kang · Z. Liu
Key Laboratory of Applied Surface and Colloid Chemistry, Shaanxi Normal University, Ministry of Education, Xi'an 710062, People's Republic of China

X. Zhang · X. Chang · N. Chen · K. Wang · L. Kang · Z. Liu (✉)
School of Materials Science and Engineering, Shaanxi Normal University, Xi'an 710062, Shaanxi, People's Republic of China
e-mail: zhliu@snnu.edu.cn

specific capacitance of 160 F g^{-1}, while the manganese dioxide thin films have a capacitance in the range between 100 and 400 F g^{-1} due to high utilization of material, which are far from the theoretical specific capacitance of $\simeq$1000 F g^{-1}. Therefore, manganese oxides with high specific capacitance, good cyclic stability, and low fabrication cost are expected.

Till now, although birnessite-type manganese oxides with different morphologies such as nanobelt [14, 15], flower-like microsphere [16], nanobundles [17], flower-like nanowhisker [18], and so on have been prepared, the obtained materials have less specific surface area (in the range between 20 and 150 m^2 g^{-1}) [19], and it limits the active material applications for supercapacitor. Thus, the research on the preparation method to create nanostructure active materials with large specific surface area is of great significance. By a templating-assisted hydrothermal process, herein hierarchical hollow manganese oxide nanosphere with both a large surface area (253 m^2 g^{-1}) and a layered structure is prepared at 150 °C for 48 h [12]. However, the synthesized process is complicate and requires relatively high hydrothermal treatment temperature. In this study, a facile low-temperature hydrothermal method is developed to synthesize δ-MnO_2 electrode active material with large surface area (188 m^2 g^{-1}) in a mixed system of potassium permanganate ($KMnO_4$) and epoxypropane (C_3H_6O) at 90 °C for 24 h, and the capacitance of the obtained material is investigated.

Experimental section

δ-MnO_2 preparation

All chemicals were of analytical grade and were used as purchased without further purification. Deionized water was used throughout the experiment.

In a typical synthesis, 4 mmol $KMnO_4$ was dissolved in 15 mL of 0.2 mol L^{-1} C_3H_6O aqueous solution under magnetic stirring for 25 min at room temperature; the mixed solution was then transferred to a 20 mL Teflon-lined stainless steel auto-clave and heated at 90 °C for 24 h. After the reaction was completed, the resulting brownish-black solid product was filtrated, washed with deionized water, and finally dried at 50 °C for 24 h in air. The effect of C_3H_6O solution concentration on the crystallinity and morphology of the obtained materials was investigated by the above same experiments.

Characterization

The powder X-ray diffraction (XRD) pattern was recorded on a D/Max-3c X-ray diffractometer with Cu Ka radiation (λ = 1.5406 Å), using an operation voltage and current of 40 kV and 40 mA, respectively. A Quanta 200 environmental scanning electron microscopy (SEM) was used to observe the morphology of the obtained materials. For TEM observation, the samples were redispersed in ethanol by ultrasonic treatment and dropped on carbon–copper grids. TEM images were collected using a JEOLJEM-3010 microscope working at 120 kV. A Beckman coulter-type nitrogen adsorption–desorption apparatus was used to investigate the pore property degassing for 6 h below 10^{-3} mmHg. Mn and K contents were determined by atomic absorption spectrometry after samples were dissolved in a mixed solution of HCl (1.0 mol L^{-1}) and H_2O_2 (28%) (v/v = 5:1).

Electrochemical measurement

Electrodes were prepared by mixing MnO_2 power (75 wt%) as active material, with acetylene black (20 wt%), and polyvinylidene fluoride (5 wt%). The two former constituents were first mixed together to obtain a homogeneous black power. The polyvinylidene fluoride solution (0.02 g mL^{-1}, in *N*-methyl-ketopyrrolidine) was then added. This resulted in a rubber-like paste, which was brush-coated onto a Ni mesh. The mesh was dried at 110 °C in air for 2 h for the removal of the solvent. After being dried, the coated mesh was uniaxially pressed to make the electrode material completely adhere with the current collector.

An IviumStat electrochemical workstation (Ivium Technologies BV, Holland) was used for electrochemical measurements. A beaker type electrochemical cell equipped with MnO_2-based working electrode, a Pt-foil (2 cm^2) as the counter electrode and saturated calomel electrode (SCE) as the reference electrode. CV curves were done between −0.2 V and 0.8 V in a Na_2SO_4 electrolyte (1 mol L^{-1}) at a sweep rate of 5 mV s^{-1}. The average specific capacitance could be accounted according to the area of the charge and discharge curves of the CV plot [20].

Results and discussion

XRD pattern of the as-synthesized material shows a series of the broad peaks, and the diffraction peaks at 12.5°, 25.0°, and 37.1° can be indexed to a typical birnessite-type manganese oxide (JCPDS 23-1046) with a basal spacing of 0.72 nm (Fig. 1a). The diffraction peaks are low in intensity, indicating the as-prepared δ-MnO_2 possesses weak crystalline. According to the element analysis results obtained by atomic absorption spectrometry, the Mn/K molar ratio is near to 5. The Mn/K molar ratio expresses the content of Mn (IΠ) and the average oxide state of

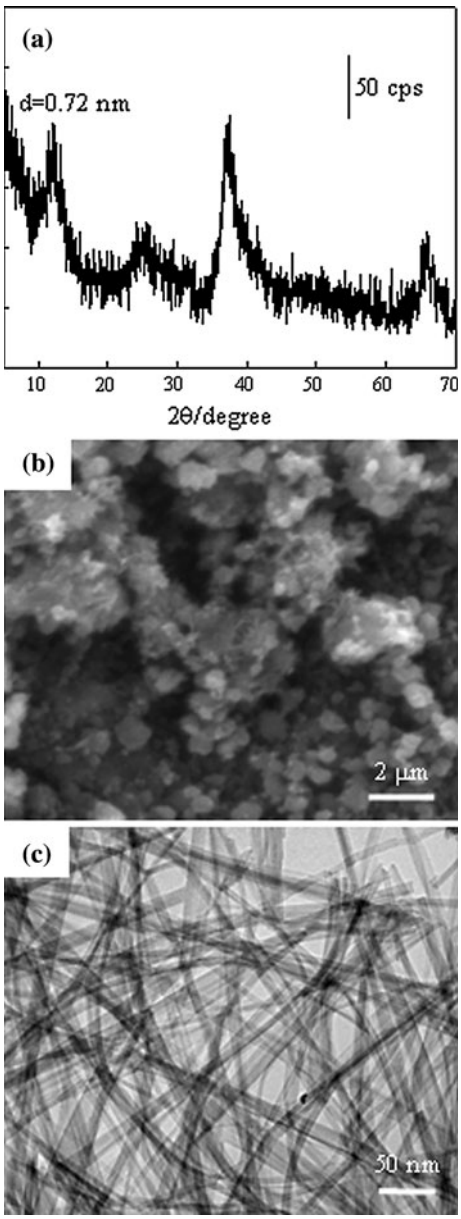

Fig. 1 XRD pattern (**a**), SEM (**b**), and TEM images (**c**) of the synthesized δ-MnO_2

manganese for the prepared material. In general, typical δ-MnO_2 has a formula of $K_4Mn_{14}O_{27}{\cdot}9H_2O$ and the Mn/K molar ratio is 3.5. In comparison with the typical δ-MnO_2, the Mn/K molar ratio is higher, suggesting that the content of Mn (III) is low and the average oxide state of manganese is high in the prepared δ-MnO_2. The as-synthesized material shows irregular overall morphology and serious particle agglomerate behavior is observed (Fig. 1b). The morphology in detail can be observed from the high magnification TEM image, and it is indicated that δ-MnO_2 prepared by the present method is dominated by the very long flexible bundles assembled with nanobelts with 10–20 nm in width and more than several micrometers in length (Fig. 1c).

The concentration of C_3H_6O solution in the reaction system has an obvious influence for the crystallinity and morphology of the obtained materials. When no C_3H_6O is added, the as-prepared material shows hardly amorphous crystalline characterization (Fig. 2a). When the concentration of C_3H_6O solution is increased to 0.2 mol L^{-1}, δ-MnO_2 with layered structure and a basal spacing of 0.72 nm is obtained (Fig. 2b). In company with the concentration increase of C_3H_6O solution, the phase of the obtained sample obviously changes into γ-MnOOH with a little β-MnOOH as impurity (Fig. 2c). Continuing to increase the concentration of C_3H_6O solution, only the crystallization of the obtained material becomes increase in intensity, but its structure hardly changes (Fig. 2d). The concentration of C_3H_6O solution not only influences the crystallinity and structure of the as-prepared materials, but also influences their morphology (supporting information Figure S1). A suitable concentration of C_3H_6O solution is favorable for the formation of δ-MnO_2 with layered structure. Without the addition of C_3H_6O in the reaction system, the as-prepared material shows aggregated sphere morphology, which are assembled with nanobelt bundles. When the concentration of C_3H_6O solution is between 0.3 and 0.6 mol L^{-1}, obvious rod morphology is observed due to the formation of γ-MnOOH phase. Irregular aggregated layered morphology is only observed when the concentration of C_3H_6O solution is 0.2 mol L^{-1}. C_3H_6O plays a role of soft template in forming

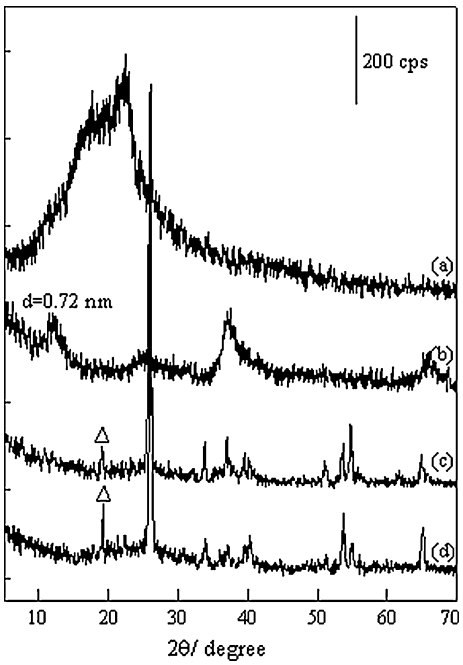

Fig. 2 XRD patterns of the obtained materials at different epoxypropane concentrations: (*a*) 0 mol L^{-1}, (*b*) 0.2 mol L^{-1}, (*c*) 0.4 mol L^{-1}, and (*d*) 0.6 mol L^{-1} (Δ, β-MnOOH)

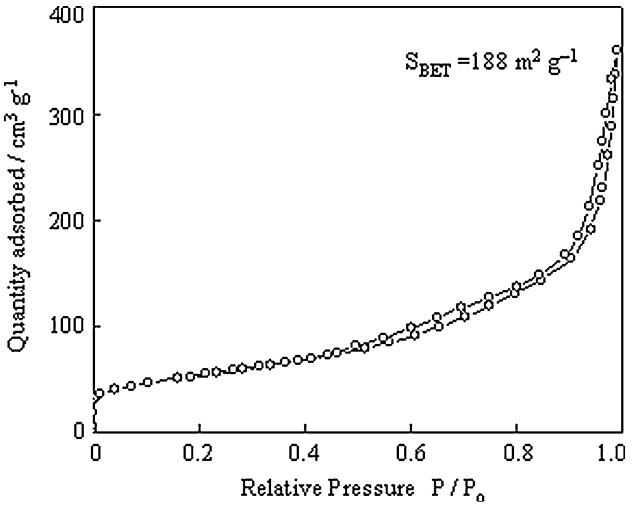

Fig. 3 N_2 adsorption–desorption isotherms of the synthesized δ-MnO_2

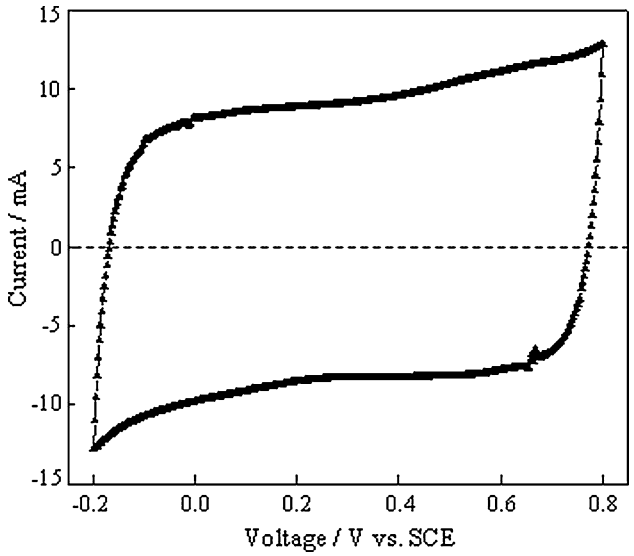

Fig. 4 The cyclic voltammogram curves of the synthesized δ-MnO_2 at a scan rate of 5 mV s^{-1} in 1 mol L^{-1} Na_2SO_4 solution

the microstructure of δ-MnO_2. A homogeneous nucleation process happens when $KMnO_4$ is hydrothermally treated, and it results in the nuclei formation from the instable $KMnO_4$ solution in high energy. The formed nuclei aggregate in virtue of the free energy of the new nuclei surface, and the aggregated nuclei acts as the seed for the formation of δ-MnO_2 due to the anisotropic habit driven by chemical potential under hydrothermal condition.

N_2 adsorption–desorption isotherms of the obtained δ-MnO_2 with layered structure exhibit type IV adsorption isotherm behavior classified by the International Union of Pure and Applied Chemistry (IUPAC) (Fig. 3) [21]. A hysteresis loop between the adsorption and desorption branches can be considered as type H3, indicating slit-like pores [22]. The obtained δ-MnO_2 with layered structure possesses a much higher BET surface area of 188 m^2 g^{-1} and larger N_2 adsorption volume. The BET surface area is larger than that reported by Wei and coworkers [18], Kang and coworkers [23], and Munichandraiah and coworker [10], in which nanostructured MnO_2 is obtained and the BET surface area is between 130 and 160 m^2 g^{-1}. BJH average pore diameter of 11.76 nm confirms the predominant presence of mesopores in the obtained δ-MnO_2 with layered structure. These results clearly indicate that the formation of the nanobelt bundles in δ-MnO_2 with layered structure drastically enhances the mesoporosity as well as the specific surface area.

Extensive studies have shown that manganese oxides are promising electrode materials for electrochemical supercapacitors. Cyclic voltammetry is an important method to investigate the capacitive behavior of the obtained δ-MnO_2 with layered structure. The CV curve obtained in a Na_2SO_4 (1 mol L^{-1}) solution at a sweep rate of 5 mV s^{-1} shows relatively rectangular mirror image with respect to the zero-current line (Fig. 4). The rectangular mirror image indicates that the obtained δ-MnO_2 with layered structure behaves obvious capacitive behavior. There are no redox peak in the range between −0.2 and 0.8 V, indicating that the δ-MnO_2 with layered structure electrode prepared by the present method is charged and discharged at a pseudo constant rate over the complete voltammetric cycle and good reversibility at this potential range [24]. The specific capacitance value (C_m) can be calculated from the CV curve according to the following equation: $C_m = \frac{i}{mv}$, where m is the total mass of active material in electrode, v is the potential sweep rate, and i is the even current response defined by $i = \left(\int_{Va}^{Vc} i(v)\mathrm{d}v\right) \Big/ (Vc - Va)$ and where Vc is cut-off voltage and Va is the initial voltage of CV curve. The specific capacitance value calculated from the cyclic voltammetry curve is found to be 296 F g^{-1}, indicating that the δ-MnO_2 with layered structure prepared by the present method behaves as good capacitor within the window of −0.2 to 0.8 V. The good electrochemical behavior is probably ascribed to the relative high amount of manganese and large BET surface area. At different potential scan rates ranging from 5 to 100 mV s^{-1} in the range of −0.2 to 0.8 V, CV cyclic voltammetry in a Na_2SO_4 solution (1 mol L^{-1}) of the obtained δ-MnO_2 with layered structure shows that the rectangular characteristic of the CV curves hardly changes at lower scan rates, indicating almost ideal capacitive behavior for the obtained materials (Fig. 5). Even if at relative high scan rate of 100 mV s^{-1}, the relatively rectangular mirror image with respect to the zero-current line is also found, indicating that the obtained δ-MnO_2 with layered structure shows high reactive activity and reversibility.

The variation of the specific capacitance as a function of cycle number shows that the specific capacitance slightly

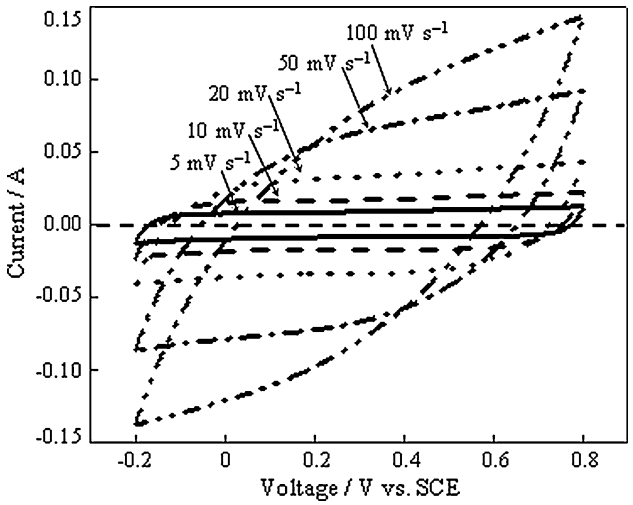

Fig. 5 CV curves of the synthesized δ-MnO_2 at various scan rates as indicated

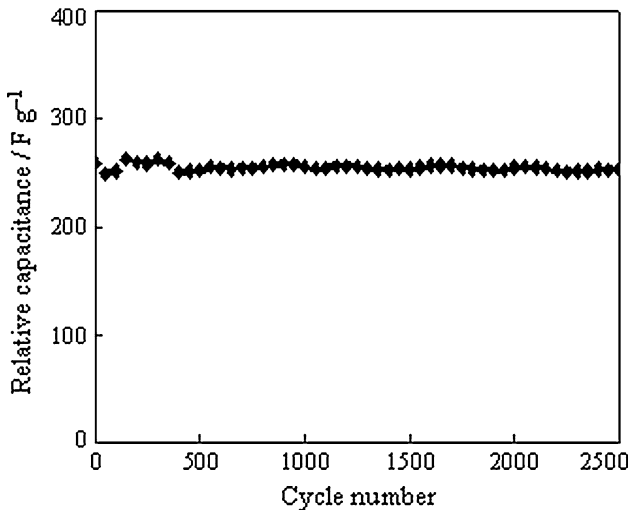

Fig. 6 Variation of the specific capacitance with respect to the cycle number in 1.0 mol L^{-1} Na_2SO_4 within a potential window ranging from −0.2 to 0.8 V versus Hg/Hg_2SO_4 at a sweep rate of 10 mV s^{-1}

decreases with the increase of the cycle number. With the scan rate of 10 mV s^{-1}, the specific capacitance value for the 1st cycle is 259 F g^{-1}, the value only decreases to 253 F g^{-1} after the 2500th cycle (Fig. 6). After the 2500 cycles of the operation, the electrode maintains 97.7% of the initial value between −0.2 and 0.8 V, indicating that the δ-MnO_2 with layered structure electrode material possesses excellent cycling stability.

Conclusions

In conclusion, δ-MnO_2 with large surface area and good capacitive property is synthesized by a facile hydrothermal method at low temperature. The obtained δ-MnO_2 has a layered structure with a basal spacing of 0.72 nm and long flexible bundles assembled with nanobelts. C_3H_6O existing in the reaction system plays a crucial role for the formation of δ-MnO_2 particles. The as-prepared δ-MnO_2 with layered structure not only possesses large area, but also shows good capacitive behavior and cycling stability in a neutral electrolyte system. This electrode material has promising application in supercapacitor because of its advantages of low cost, high capacitance, and good cycling stability.

Acknowledgements We thank National Natural Science Foundation of China (20971082) and the Natural Science Key Foundation of Shaanxi Province (2011JZ001) for financial support for this research.

References

1. Yan D, Yan PX, Cheng S, Chen JT, Zhuo RF, Feng JJ, Zhang GA (2009) Cryst Growth Des 9:218
2. Nagarajan N, Cheong M, Zhitomirsky I (2007) Mater Chem Phys 103:47
3. Beaudrouet E, Salle ALGL, Guyomard D (2009) Electrochim Acta 54:1240
4. Tian ZR, Tong W, Wang JY, Duan NG, Krishnan VV, Suib SL (1997) Science 276:926
5. Yan J, Fan ZJ, Wei T, Qian WZ, Zhang ML, Wei F (2010) Carbon 48:3825
6. Ma SB, Nam KW, Yoon WS, Yang XQ, Ahn KY, Oh KH, Kim KB (2008) J Power Sour 178:483
7. Komaba S, Ogata A, Tsuchikawa T (2008) Electrochem Commun 10:1435
8. An GM, Yu P, Xiao MJ, Liu ZM, Miao ZJ, Ding KL, Mao LQ (2008) Nanotechnology 19:275709
9. Yu P, Zhang X, Wang DL, Wang L, Ma YW (2009) Cryst Growth Des 9:528
10. Devaraj S, Munichandraiah N (2008) J Phys Chem C 112:4406
11. Luo JY, Cheng L, Xia YY (2007) Electrochem Commun 9:1404
12. Tang XH, Liu Z-H, Zhang CX, Yang ZP, Wang ZL (2009) J Power Sour 193:939
13. Wei WF, Cui XW, Chen WX, Ivey DG (2011) Chem Soc Rev 40:1697
14. Ma RZ, Bando Y, Zhang LQ, Sasaki T (2004) Adv Mater 16:918
15. Liu ZP, Ma RZ, Ebina Y, Takada K, Sasaki T (2007) Chem Mater 19:6504
16. Zhang LC, Kang LP, Lv H, Su ZK, Ooi K, Liu Z-H (2008) J Mater Res 23:780
17. Ge JC, Zhuo LH, Yang F, Tang B, Wu LZ, Tung C (2006) J Phys Chem B 110:17854
18. Subramanian V, Zhu HW, Wei BQ (2006) J Power Sour 159:361
19. Subramanian V, Zhu HW, Vajtai R, Ajayan PM, Wei BQ (2005) J Phys Chem B 109:20207
20. Yuan CZ, Gao B, Zhang XG (2007) J Power Sour 173:606
21. Kruk M, Jaroniec M (2001) Chem Mater 13:3169
22. Xu RR, Pang WQ (2005) Chemistry—zeolites and porous materials. Science Press, Beijing
23. Xu CJ, Li BH, Du HD, Kang FY, Zeng YQ (2008) J Power Sour 180:664
24. Yuan JQ, Liu Z-H, Qiao SF, Ma XR, Xu NC (2009) J Power Sour 189:1278